Acid and Iron Experimental Evolution of *Halobacterium* sp. NRC-1

by

Karina S. Kunka,[a] Jessie M. Griffith,[a] Chase Holdener,[a] Katarina M. Bischof,[a] Haofan Li,[a] Priya DasSarma,[b] Shiladitya DasSarma,[b] and Joan L. Slonczewski[a#]

[a]Department of Biology, Kenyon College, Gambier, Ohio, USA.

[b]Institute of Marine and Environmental Technology, Department of Microbiology and Immunology, University of Maryland School of Medicine, Baltimore, Maryland, USA

[#]Corresponding Author:

Joan L. Slonczewski, slonczewski@kenyon.edu

Department of Biology, Kenyon College, Gambier, Ohio, USA

ABSTRACT

Halobacterium sp. NRC-1 (NRC-1) is an extremely halophilic archaeon that is well adapted to multiple stressors such as UV, ionizing radiation, and arsenic exposure. We conducted experimental evolution of NRC-1 under acid and iron stress to expand the stressors. NRC-1 was serially cultured in CM+ medium modified by four stress conditions, with four evolving populations per condition. At 500 generations the conditions were: optimal pH (pH 7.5), acid stress (pH 6.3), iron stress (600 μM ferrous sulfate, pH 7.5), and acid plus iron stress (600 μM ferrous sulfate, pH 6.3). 16 clones from the 500th generation were isolated and characterized for phenotypic changes, and the genomes of the evolved clones were sequenced. Genotypic analysis of all 16 clones revealed 378 mutations, with patterns of high variability arising from movement of insertion sequences (ISH elements) and large deletions. One minichromosome (megaplasmid) pNRC100 had increased copy number. The 500-generation clones had frequent loss of gas vesicles and arsenic resistance. An acid-evolved clone had increased fitness compared to the ancestral stock, when cultured at low pH. Seven of eight acid-evolved clones had a mutation in or upstream of *nhaC3*, encoding a sodium-proton antiporter that exports sodium and takes in protons; no non-acid adapted strains had *nhaC3* mutations. Two acid-adapted strains shared a common mutation in *bop*, encoding the bacteriorhodopsin light-driven proton pump. Mutations also affected the *arcR* regulator of arginine catabolism, which can mediate proton transport. Thus, in the haloarchaeon NRC-1, as in bacteria, pH adaptation was associated with genes affecting proton transport.

IMPORTANCE

Thus far, few studies of experimental evolution have been conducted in archaea. Haloarchaea are polyextremophiles capable of growth under environmental conditions such as concentrated NaCl, high doses of ionizing and UV irradiation, and desiccation. *Halobacterium*

sp. NRC-1 (NRC-1) is considered a model organism for the feasibility of microbial life on Mars. Our experimental evolution of NRC-1 adaptation to iron and acid stress may yield clues as to how microbes could adapt to the ancient Martian conditions of iron-rich, acidic brine. Interesting parallels were found between the molecular basis of pH adaptation in NRC-1 and in bacteria.

INTRODUCTION

Halobacterium sp. NRC-1 (NRC-1) is a polyextremophile that grows optimally at NaCl concentrations in excess of 4 molar (1). A genetically tractable model microbe (2), it was the first halophilic Archaeon with a fully sequenced genome (3). Besides high salt, NRC-1 is capable of surviving high doses of ionizing radiation and dessication (4), UV radiation (5), temperature extremes (6), and toxic ions such as arsenite (7). These traits have made NRC-1 a model for studying the possibility of life on Mars (8–10), by subjecting cells to stressors in the laboratory and environmental conditions such as the stratosphere (11, 12).

Water on Mars contains high concentrations of salt, as well as acid and iron (13). The Mars Exploration Rover Opportunity discovered substantial deposits of an iron hydrous sulfate mineral known as jarosite [$KFe^{3+}_3(OH)_6(SO_4)_2$] which on Earth forms in acidic and iron-rich aqueous environments such as acid mine drainage and near volcanic vents. Opportunity's discovery of jarosite on Mars was evidence of acidic, liquid water and an oxidizing atmosphere in the Martian past (13, 14). Acid and metals can amplify the stress associated with each condition (15). It is of interest to investigate how a neutralophilic halophile such as NRC-1 (16) might adapt to acid and iron stress.

An informative approach to examine the genomic basis of stress response is experimental laboratory evolution (17–23). Experimental evolution of bacteria reveals changes in phenotype and genotype in response to specific stressors in a controlled environment, such as carbon source limitation or extreme pH. In bacterial adaptation to various kinds of pH stress, we find a recurring pattern that dominant responses to short-term stress actually decrease fitness over many generations of long-term exposure. For example, amino-acid transport and catabolism play important roles in extreme-acid survival of *Escherichia coli* (24, 25). But 2,000 generations of *E.*

coli evolution at pH 4.8 select for loss of three acid-inducible amino-acid decarboxylase systems (21). A membrane-permeant acid, benzoic acid induces glutamate decarboxylase and drug resistance regulons; yet these systems are lost or downregulated during experimental evolution (Moore et al. 2019 AEM00966-19) (20). At high external pH, *E. coli* survival requires the stress sigma RpoS; yet generations of growth at high pH selects against RpoS expression and activity (26). It was of interest to see whether similar patterns of reversal are found in archaea.

Relatively few experimental evolution studies have been reported in archaea. In NRC-1, serial killing doses of ionizing radiation led to more tolerant mutants with upregulation of a single-stranded DNA binding protein operon (27). In the thermoacidophile *Sulfolobus solfatericus*, serial passage in extreme acid yielded strains that grow below pH 1 (28). These strains showed mutations in amino acid transporters, as well as upregulation of membrane biosynthesis and oxidative stress response. In *Metallosphaera sedula*, serial passage led to a pH 0.9-adapted strain with four mutations, one of which is an amino-acid/polyamine transporter (29). These findings are intriguing, given the role of amino-acid transport and catabolism in extreme-acid survival of bacteria (24, 25).

In archaea and in bacteria, various pH responses involve proton transport via primary pumps as well as antiporters (24, 30, 31). *Halobacterium* strains possess a light-driven proton pump, bacteriorhodopsin, that generates proton motive force (PMF) (32, 33). NRC-1 has five sodium-proton antiporters, which export sodium in exchange for protons (6). In alkaliphilic *Bacillus* species (34) and in *Escherichia coli* (35) sodium-proton antiporters mediate responses to high pH.

We conducted experimental evolution of NRC-1 under conditions of high iron versus low iron, at low pH (pH 6.5-6.3) and at optimal pH for growth (pH 7.5). The NRC-1 genome

92 includes a main chromosome and two minichromosomes or megaplasmids (3, 36) . It
93 accumulates frequent IS mutations (37, 38) which may mediate rapid adaptations to
94 environmental stress. Our study of experimental evolution in a haloarchaeon assesses which
95 mutations contribute to archaeal evolution in iron and acid stress. Here we describe analysis of
96 phenotypic changes across evolved clones from each population in gas vesicle formation,
97 motility, and growth under the four conditions, and then use genomic analysis to identify
98 potential underlying mutational bases of these phenotypic responses to selection. Genome
99 analysis of 16 clones revealed numerous insertions and deletions mediated by insertion
100 sequences (ISH). Of special interest, we identify two loci whose mutations occur in acid-adapted
101 strains, namely *nhaC* (Na^+/H^+ antiporter) (6) and *bop* (bacteriorhodopsin) (32, 33).

RESULTS

Experimental evolution under conditions of acid and iron stress. Serial culture of evolving populations was conducted as described under Methods. Populations of NRC-1 were founded from a single clone and cultured in modified CM^+ medium (2, 3) with appropriate buffers to maintain pH. Each population was diluted 500-fold every four days (approximately 9 generations). Four independent populations were maintained for each condition: the optimal growth condition, pH 7.5 (designation M); acid stress, initially pH 6.5, later pH 6.3 (designated J); iron stress, pH 7.5 amended with 600 µM ferrous sulfate (designated S); and acid with iron amendment (designated K) for a total of 16 experimental populations. Populations evolved under acid stress were cultured at an initial pH of 6.5, which was then lowered to 6.3 as the populations adapted, at generation 250.

After reaching 500 doublings, two clones were isolated from each population by three rounds of streaking on CM+ agar for a total of 32 evolved clones. Genomic DNA was extracted from 16 of these clones, and from the founder stock of NRC-1. DNA samples were sequenced by Illumina MiSeq, and mutations were identified by comparison of the "evolved strain" sequences to that of the NRC-1 ancestral stock, assembled on the reference genome (3) using the *breseq* pipeline (39–41). The strains we characterized are listed in **Table 1**.

Mutations in the genomes from evolving populations. The genomes of the 16 clones were compared to those of the resequenced NRC-1 ancestor (**Tables S1, S2, S3**). The genomes of the evolved clones had a total of 378 mutations, of which 349 were unique to one strain at the base-pair level. Representative mutations of interest are summarized in **Table 2**. The genome of our ancestral NRC-1 stock was also compared to that of the NCBI reference (3) as shown in

125 **Table S4**; the differences between these sequences were excluded in our analysis of the evolved
126 clones.

127 In the 16 clones, overall, 87 mutations were found on the main chromosome. There were
128 120 mutations in minichromosome pNRC100, and 171 mutations on minichromosome
129 pNRC200. pNRC100 is about 10% as long as the main chromosome, and pNRC200 is about
130 20% as long; thus, the two minichromosomes had a mutation frequency more than ten-fold
131 greater than that of the main chromosome, a finding consistent with previous reports of plasmid
132 mutation (3). The main chromosome and the two minichromosomes had numerous target site
133 duplications (TSDs) caused by ISH element insertions (37), as well as large deletions also
134 mediated by ISH mobility (**Table 3**) (42–45). For comparison, in *E. coli* the mutations selected
135 under stress conditions often originate via insertion elements (20). In haloarchaea, ISH elements
136 are even more active and cause numerous large-scale mutation events (46).

137 Haloarchaea including *Halobacterium salinarum* species are known for polyploidy (15-
138 25 genome copies per cell) and for ploidy variation among replicons within a cell (47). Our
139 evolved clones showed evidence for variable ploidy between and within replicons. Mean read
140 coverage by replicon was modeled by *breseq* (**Table 4**). Overall, within the ancestor and the
141 evolved clones, the read coverage for the main chromosome was consistent with that of the
142 minichromosome pNRC200. However, the mean coverage of the shorter minichromosome
143 pNRC100 (191 kb) was more than twice that of the main chromosome, for our ancestral NRC-1
144 and for 12 of the 16 evolved clones. Clones J1, M3-1, K3, S2, and S3 had mean coverage of
145 pNRC100 more than four-fold greater than that of the main chromosome. These high coverage
146 ratios could indicate that our original NRC-1 stock has a double copy number of
147 minichromosome pNRC100, relative to the main chromosome; and that some descendant clones

have increased relative copy number. However, the calculations are complicated by wide variation in read coverage between different segments of the same replicon, especially in pNRC100, likely due to internal repeats in the replicon (35). Interpretation of the data is also complicated by the presence of massive deletions (**Table S2**) which comprise up to 50% of the ancestral sequence (for example in clone K1) (45). Variation in read coverage could indicate the presence of plasmid copies with different deletion levels within a given polyploid cell.

Multiple clones lost gas vesicles and arsenic resistance. Under laboratory conditions, a gas vesicle-producing (Vac^+) NRC-1 clones have high rates of spontaneous mutation to a vesicle-deficient (Vac^-) phenotype due to mutations in *gvp* on pNRC100 (37, 42). 12/16 of our evolved clones, including members of all four selection classes, had lost genes required for gas vesicle nanoparticle production (*gvp*) (48–50). Cultures were oxygenated continually by rotating in a bath, effectively eliminating the competitive advantage of producing gas vesicles in oxygen-limiting environments. Thus, as expected, many insertions and deletions were found that had eliminated gas vesicles (42, 46). We characterized gas vesicle phenotypes every 100 generations for the stressed condition populations. These Vac phenotypes (loss of gas vesicle nanoparticles) are presented by population and organized by respective evolution condition in **Table 7.** All evolving populations showed loss of gas vesicle production in some cells. By generation 500, the Vac^- phenotype was prevalent in all populations. There was no significant correlation with pH or with iron amendment.

In addition, 13/16 evolved clones had lost the major arsenic resistance operon (*ars*) encoded on pNRC100 (7). Other mutations affecting transcriptional regulators and initiation factors occurred in parallel across multiple populations. These and other parallel mutations are

summarized in **Table 2**, in which apparent "hot spots" for mutation are grouped based on the degree of parallelism observed.

Acid-evolved clone J3-1 has a growth advantage over a range of pH values. The clones after 500 generations of serial culture under four conditions were tested for genetic adaptation under various growth conditions. Each evolved clone was cultured in parallel with the ancestral strain NRC-1. The loss of gas vesicles (Vac^- phenotype) alters their OD_{600} reading (37, 42); for this reason, clones that had lost gas vesicles were cultured in parallel with a Vac^- isolate of NRC-1 ancestor.

The growth of acid-evolved J-population clones was compared to that of the NRC-1 ancestor (Vac^+) (**Figs. 1 and 2**). Clone J3-1 reached a significant two-fold higher culture density than did the ancestor, cultured at pH 6.1 or at 6.3 (**Fig. 1B**). Growth advantage was seen for all four replicate cultures of J3-1 at pH 6.1 and at pH 6.3, whereas the difference from NRC-1 cultures disappeared at pH 7.2 and at pH 7.5. Thus, strain J3-1 exhibits an acid-specific fitness advantage. The other acid-evolved J-population strains, however, had no significant growth advantage compared to NRC-1, under the conditions tested (**Fig. 2**).

Acid-adapted clones shared mutations in *nhaC3*, in *bop*, and in *arcR*. We inspected the genomes of acid-adapted populations J and K (acid with iron supplement) for mutations in specific genes that were not found in the populations evolved at pH 7.5. Seven out of eight of the J and K clones (but no M or S clones) had target site duplications in or upstream of the Na^+/H^+ antiporter, *nhaC3*, observed by *breseq* and suggestive of an IS element (**Table 2**). PCR amplification and Sanger sequencing of the mutant *nhaC3* alleles confirmed the presence of insertion sequences ISH2 (strains K1 and K4) and ISH4 (strains J1, K2-1, K3) (**Table 5**; **Fig. S2**). Additionally, in J4-2, a partial sequence confirms the presence of 1.1 kb ISH11 insertion

193 flanked by a 10 bp direct repeat, while a large, 3000+ bp insertion in K3 returned a partial
194 sequence of ISH4 (**Fig. S2**). The partial sequence suggests multiple copies of ISH4, or possibly a
195 composite transposon.

196 Clones J3-1 and K1 each contained a target site duplication in the gene *bop* that encodes
197 the light-driven proton pump (bacteriorhodopsin) (32). The J3-1 allele was confirmed by Sanger
198 sequence as a 1.1 kb insertion of ISH1 with an eight bp target site duplication in *bop* (**Table 5**;
199 **Fig. S2**). This exact mutation has been previously studied in bacteriorhodopsin mutants, and was
200 in fact the first transposable element identified in haloarchaea (32). This particular target site
201 duplication was shared with acid-evolved clone K1. At a different position, a *bop* ISH insertion
202 was found in one of the M population clones (M3-1) which had not undergone acid selection,
203 consistent with previous spontaneous insertions in this gene.

204 The *bop* and *nhaC3* mutations were found together in J3-1, but also in acid-adapted K1,
205 which did not show a significant phenotype under our conditions tested. We inspected strain J3-1
206 for candidate mutations that might be responsible for this strain's unique degree of adaptation at
207 low pH. Overall, the J3-1 genome had 16 mutations compared to the NRC-1 ancestor (**Table 6**).
208 Of these, only one mutation affected a gene not affected in any other evolved clone. This is a
209 missense mutation in a ferredoxin gene (*vng1561*) resulting in a conservative change from lysine
210 to arginine. Mutations were also found affecting several proteins involved in transcriptional
211 regulation, which in particular combination might contribute to the acid fitness phenotype.

212 Four acid-evolved genomes (J-3, K-1, K2-1, K4-1) and one non-acid-evolved clone (M3-
213 1) possess TSDs at different sites in *arcR* on pNRC100 (**Table S3**). ArcR mediates
214 transcriptional regulation of the *arcABDCR* operon for arginine catabolism (51, 52). In *E. coli*,
215 the arginine decarboxylase Adi consumes a proton, reversing acidification (53). The *adi* system

is induced by acid stress but largely lost after long-term acid evolution (20, 22). This would imply a model for acid adaptation in haloarchaea that is remarkably similar to that observed in *E. coli*, in which acid-stress adaptations are knocked down by long-term acid exposure (21).

Clones evolved at pH 7.5 show no increase in relative fitness. All evolved clones from generation 500 with Vac^- phenotypes were grown over 200 hours in unbuffered CM^+ medium without acid or iron amendment and compared to the growth phenotype of the NRC-1 Vac^- control strain (**Fig. S2A**). Similarly, the growth phenotypes in unstressed medium of Vac^+ clones from the 500-generation populations that retained them were compared to that of the NRC-1 Vac^+ ancestor (**Fig. S2B)**. None of the M populations show a significant growth advantage compared to the ancestral strain (**Fig. S3A and B**).

Growth curves were also conducted for clones from the S populations (evolved with 600 μM $FeSO_4$). Media contained CM+ pH 7.5 with 100 mM MOPS and 600 μM $FeSO_4$. All evolved clones were persistent Vac^- mutants at generation 500 and are thus compared to an NRC-1 Vac^- control (**Fig. S4**). No significant differences were observed.

DISCUSSION

Here we report one of the first evolution experiments on a haloarchaeon; a previous experiment involved selection of mutants resistant to ionizing radiation (27). We compared four environmental conditions: low pH versus optimal pH 7.5, with or without iron supplementation. Overall, in the 500-generation evolved strains, we found a striking pattern of large ISH-mediated deletions, particularly in the two minichromosomes (**Table S1-S3**). For comparison, in *E.* coli, experimental evolution for 2,000 generations at low pH yields only occasional large deletions (20, 21). However, in the haloarchaeon NRC-1 after just 500 generations every evolved clone contained several large-scale deletions. ISH insertion mutations greatly outnumbered SNPs. These types of changes reflect frequent DNA rearrangements and genetic variability observed previously in NRC-1 (32, 38, 44).

The acid-adapted NRC-1 populations showed a striking prevalence of mutations affecting the NhaC3 Na^+/H^+ antiporter. While NhaC3 is useful for expelling excess Na^+, its long-term function at low pH the proton gradient could over-drive the system, perhaps acidifying the cytoplasm. For comparison, in *E. coli*, experimental evolution with the PMF-depleting uncoupler carbonyl cyanide m-chlorophenylhydrazone (CCCP) leads to mutation in an *nha* ortholog (54).

In addition, the acid-evolved strains J3-1 and K1 show an identical insertion mutation affecting *bop* bacteriorhodopsin. The loss of *bop* may be neutral or advantageous under low external pH, where a high proton motive force already exists. The bacteriorhodopsin pump could be a source of proton leakage at high PMF.

Another mutant gene in acid-evolved clones was the *arcR* mediator of arginine catabolism and arginine-ornithine transport. A comparable arginine catabolism system in *E. coli* exports protons under acid stress, yet is lost during acid evolution (20, 51). The reason for the

255 evolutionary loss is proposed to be a readjustment to long-term acid exposure, for which the
256 sustained induction of arginine catabolism becomes counterproductive.

257 The acid-fitness advantage of clone J3-1 could arise from a single mutation unique to J3-
258 1, such as the missense mutation in a ferredoxin that is unique to J3-1. More likely, however,
259 acid fitness arises from a cumulative effect of loss of function mutations in a number of other
260 genes. The J3-1 and K1 acid-evolved clones both possess insertions in *nhaC3*, *bop*, and *arcR*. It
261 is possible that some other factor we missed makes the difference for J3-1 showing an acid-
262 fitness phenotype under the conditions tested. Nonetheless, it is interesting that the three genes
263 showing mutations in multiple acid-evolved strains all encode products involved in proton
264 export. This finding is remarkably consistent with the multiple reports in *E. coli* that long-term
265 exposure to pH stress leads to loss of proton exchange and other systems that protect cells from
266 short-term pH stress (21, 26) (Moore et al. 2019 AEM00966-19).

267 Our findings support previous reports of the importance of ISH elements in haloarchaeal
268 evolution (46), and the observations in *Sulfolobus* that large deletions and loss of function
269 mutations are fitness tradeoffs for surviving in stressful environments (55). Large deletions and
270 IS insertions are also common in experimental evolution of bacteria (20, 21, 26, 54). We also
271 find evidence for accumulation of ploidy changes for the shorter minichromosome, pNRC100
272 (47). We show that experimental evolution is an effective approach to identify candidate genes
273 for environmental stress response in a haloarchaeon.
274

MATERIALS AND METHODS

***Halobacterium* strains and media.** All evolved clones were derived from a stock of *Halobacterium sp.* NRC-1 from the laboratory of Shiladitya DasSarma (3). Liquid cultures were grown in Complex Medium Plus Trace Metals (CM^+) based on Ref (2), Protocol 25: 250 g/l NaCl, 20 g/l $MgSO_4$•$7H_2O$, 2 g/l KCl, 3 g/l $Na_3C_6H_5O_7$ •$2H_2O$, 10 g/l Oxoid Peptone, and 100 µl/l Trace Metals (3.5 g/l $FeSO_4$·$7H_2O$, 0.88 g/l $ZnSO_4$•$7H_2O$, 0.66 g/l $MnSO_4$•H_2O, and 0.2 g/l $CuSO_4$•$5H_2O$ dissolved 0.1M HCl) with supplements as needed for the conditions examined (56). CM^+ solid medium included addition of 20 g/l granulated agar. All cultures were incubated at 42˚C with rotation. Cultures on solid media were incubated at 42˚C for 7–10 days until colonies reached approximately 1 mm in diameter. A Vac^- mutant of our NRC-1 stock culture was obtained by picking a Vac^- colony followed by three restreaks on CM^+ agar.

Liquid CM^+ media for experimental evolution was made with either 100mM PIPES (pKa=6.8) or 100mM MOPS (pKa=7.2) buffer with pH adjusted using 5 M NaOH or 5 M HCl as needed, followed by filter sterilization. 100 mM $FeSO_4$ stock was prepared in deionized water and filter-sterilized before every other dilution during serial batch culture evolution. Sterilized $FeSO_4$ stock was added to buffered CM^+ after filter sterilization. For freezer stocks, live cultures were mixed 1:1 with a 50% glycerol, 50% complex medium basal salts mixture as a cryoprotectant. Complex medium basal salts were 250 g/l NaCl, 20 g/l $MgSO_4$•$7H_2O$, 2 g/l KCl, 3 g/l $Na_3C_6H_5O_7$•$2H_2O$. Acidic, control, iron-rich and acidic, and iron-rich media used in the evolution consisted of: CM^+ pH 6.5 with 100 mM PIPES (populations J1-J4), CM^+ pH 7.5 with 100 mM MOPS (populations M1-M4), CM^+ pH 6.5 (or pH 6.3) with 100 mM PIPES 600 µM $FeSO_4$ (populations K1-K4), and CM^+ pH 7.5 with 100 mM MOPS 600 µM $FeSO_4$ (populations S1-S4).

Experimental evolution. A total of 16 populations (four per evolution condition) were founded from a 5 ml CM^+ tube culture (7-10 days incubation) of *Halobacterium sp.* NRC-1 that was diluted 500-fold and incubated 4 days in a 42ºC shaker bath at 200 rpm. At the end of the fourth day, 10 µl of the previous culture was diluted into 5 ml of fresh CM^+ media amended as necessary for the respective stress condition. The resulting 1:500 dilutions yield approximately nine generations per dilution cycle. If cultures did not reach a healthy cell density as qualitatively evaluated for each dilution, 1:100 or 1:250 dilutions were performed to prevent loss of evolving populations. Alternative dilution concentrations were factored into total generation counts at the end of experimental evolution. When evolution was interrupted, the populations were revived by 1:250 dilutions from freezer stocks of the previous dilution. Freezer stocks comprised 1 ml liquid, mature haloarchaea culture for each evolving population and 0.5 ml glycerol/basal salts mixture, stored in 2 ml Wheaton brand vials and frozen at -80ºC for each dilution, totaling 16 freezer stocks every four days. A summary of the evolution procedure is presented in **Figure S1**.

Clone selection. Clones were isolated by plating 10 µl of culture from generation 100, 200, 300, 400, and 500 from freezer stocks for all 16 evolving populations on CM^+ agar plates, followed by incubation in a sealed container at 42ºC for 7–10 days. Isolated colonies were then selected for diverse Vac phenotypes, streaked on fresh CM^+ agar plates, and incubated a second time. The process was repeated a third time to ensure isolation of select genetically pure clones. Colonies from the third streak were grown in unbuffered CM^+ pH 7.2, and stocks were frozen for later phenotype and genotype characterization. One clone was isolated from each population every 100 generations. For populations that presented mixed gas vesicle production phenotypes, we isolated both a Vac^+ clone and a Vac^- clone. In total, 75 clones were isolated from generation 100, 200, 300, and 400 of the evolution. Clones were similarly isolated from generation 500, but

the first streak was taken directly from evolving populations, rather than frozen Wheaton vials. Two clones were isolated from each population at 500 generations, for a total of 32 clones.

Gas vesicle formation phenotype analysis. Vesicle formation phenotype was assessed qualitatively based on the relative translucence of plated colonies and denoted as Vac^+ or Vac^- as appropriate (2, 42). If more than one Vac phenotype was observed in a streak during strain isolation, the phenotypic variant colonies were re-streaked and treated as separate clonal isolates. Vac phenotypes were evaluated for persistence with each streak based on whether or not Vac^+ colonies yielded >1% Vac^- progeny or vice versa.

Growth assays. The generation 500 clones used in these assays are summarized in **Table 1**. Clones were cultured in unbuffered CM+ at pH 7.2, and incubated for four days in a 42ºC shaker bath with 200 rpm orbital aeration. Overweek starter cultures were diluted 1:1000 into new test tubes with 5 ml of the appropriate test condition media. A media blank was included for each media condition, and each clone was tested with four to eight biological replicates, depending on the assay. Immediately after inoculation, OD_{600} values were recorded by a Spectramax 384+ spectrophotometer at 600 nm using Softmax Pro version 6.4.2. Daily readings were taken for nine days. Media for these tests included CM+ pH 6.3 100 mM PIPES and CM+ pH 6.1 100 mM PIPES for J clones. M clones were tested in CM+ pH 7.5 100 mM MOPS. K clones were tested in CM+ pH 6.3 100 mM PIPES 600 µM $FeSO_4$ and CM+ pH 6.1 100 mM PIPES 600 µM $FeSO_4$. S clones were tested in CM+ pH 7.5 100 mM MOPS 600 µM $FeSO_4$.

To test for pH-dependent growth advantages, evolved clones that showed growth advantages over ancestor in their respective evolution stress conditions under which they were evolved were also tested for growth advantages in pH conditions other than those in which they evolved. For these experiments, J3-1 was cultured in CM+ pH 7.5 100 mM MOPS and compared

using a Vac^+ NRC-1 control, M3-1 was cultured in CM+ pH 6.1 100 mM PIPES and compared using a Vac^+ NRC-1 control, and K2-1 was cultured in CM+ pH 7.5 100 mM MOPS 600 µM $FeSO_4$ and compared to both Vac^+ and Vac^- NRC-1 controls due to gas vesicle phenotype ambiguity. Analysis was carried out with comparisons to an ancestral control expressing the same Vac phenotype as the evolved clone.

All growth assays were evaluated for statistical significance using ANOVA test with Tukey post-hoc or paired T-test using base R and agricolae package. Comparisons between clones were made using post log-phase endpoint "E" values for optical density at six days post inoculation.

DNA extraction and genome sequencing. Genomic DNA was isolated from the 16 evolved clones and the ancestor NRC-1 using an Epicentre MasterPure Gram Positive DNA Extraction Kit and a modified procedure. Lysozyme was omitted, and DNA purity and concentration was determined using a Thermo Scientific NanoDrop 2000. Genomic DNA was sequenced at the Michigan State University Research Technology Support Facility (RTSF) Genomics Core. Libraries were prepared using the Illumina TruSeq Nano DNA library preparation kit for Illumina MiSeq sequencing and loaded on a MiSeq flow cell after library validation and quantitation. Sequencing was completed using a 2- by 250-bp paired-end format using Illumina 500 cycle V2 reagent cartridge. Illumina Real Time Analysis (RTA) v1.18.54 performed base calling, and the output of the RTA was demultiplexed and converted to FastQ format with Illumina Bcl2fastq v1.8.4.

Sequence assembly and analysis using the *breseq* computational pipeline. The computational pipeline *breseq* version 0.27.1 was used to assemble and annotate the resulting Illumina reads of the evolved clones (39–41). The current *breseq* version is optimized to detect

IS element insertions and IS-mediated deletions, as well as SNPs and other mutations in *E. coli* (19). Illumina reads were mapped to the *Halobacterium sp.* NRC-1 reference genome (NCBI GenBank assembly accession GCA_000006805.1). Mutations were predicted by *breseq* through sequence comparisons between the evolved and ancestral clones.

The Integrative Genomics Viewer (IGV) from the Broad Institute at Massachusetts Institute of Technology was used to visualize the assembly and mutations in the evolved clonal sequences mapped to the reference NRC-1 genome (57). Each replicon was mapped separately using the following RefSeq IDs: NC_002607.1 (main chromosome), NC_001869.1 (pNRC100), and NC_002608.1 (pNRC200). Sequence mean coverage in each evolved clone was estimated using the *breseq* fit dispersion function.

PCR confirmation of ISH insertions. PCR primers (Table 5) were designed to confirm the presence of insertion sequences at hypothetical target site duplications. Primers adhered to the following specifications using Sigma Aldrich Oligo Evaluator: 19-22 bp in length, GC content between 40-60%, no single bp runs >3, weak to no secondary structure, and no primer dimer. Oligos were checked for sequence identity of ≤13 bp to any part of the NRC-1 genome other than the target site using NCBI BLAST. We ran 50-µl PCR using Applied Biosystems Amplitaq Gold 360 Master Mix according to the package insert with 50 µl reaction containing GC enhancer. To assess insert length, 10 µl of PCR product was electrophoresed in a 1% agarose gel. PCR products were then purified either by Qiagen QIAquick PCR Purification Kit or QIAquick Gel Extraction Kit.

Accession number for sequenced genomes. Sequenced genomes are deposited under SRA accession number SRP195828.

391 ACKNOWLEDGEMENTS

392 This project was supported by the National Science Foundation award MCB-1613278 to
393 Joan Slonczewski; by the 2016 NASA Astrobiology Program Early Career Collaboration Award
394 to Karina Kunka and Jessie Griffith; and by NASA Exobiology grants NNX15AM07G and
395 NNH18ZDA001N to Shiladitya DasSarma.

396

397

398 TABLES AND FIGURES
399

400 **Table 1. Strains used in this study**

Strain Name	Description	Generation	Evolution Condition	Vac +/- *	Source
NRC-1	Ancestor strain	0	--	+	S. DasSarma
NRC-1	Ancestor strain	0	--	-	S. DasSarma
JLSHA075	Clone J1	500	pH 6.3 100 mM PIPES	-	This study
JLSHA078	Clone J2-2	500		-	This study
JLSHA079	Clone J3-1	500		+	This study
JLSHA082	Clone J4-2	500		-	This study
JLSHA083	Clone M1	500	pH 7.5 100 mM MOPS	-	This study
JLSHA086	Clone M2-2	500		-	This study
JLSHA087	Clone M3-1	500		+	This study
JLSHA089	Clone M4-1	500		+	This study
JLSHA091	Clone K1	500	pH 6.3 100 mM PIPES 600 µM Fe^{2+}	-	This study
JLSHA093	Clone K2-1	500		+	This study
JLSHA095	Clone K3	500		-	This study
JLSHA097	Clone K4	500		-	This study
JLSHA099	Clone S1	500	pH 7.5 100 mM MOPS 600 µM Fe^{2+}	-	This study
JLSHA101	Clone S2	500		-	This study
JLSHA103	Clone S3	500		-	This study
JLSHA105	Clone S4	500		-	This study

401 *"+" indicates gas vesicle-forming, "-" indicates non gas vesicle-forming

Table 2. Selected mutations found in evolved clones.*‡

Replicon	Start bp	Mutation	J1	J2-2	J3-1	J4-2	M1	M2-2	M3-1	M4-1	K1	K2-1	K3	K4	S1	S2	S3	S4	Annotation	Gene Description
Chromosome	~15,266	TSD																	TSD: intergenic	Starts after *vng18* and ends before *vng19*.
Chromosome	~23,074	TSD																	TSD: intergenic	Starts after *vng27* and ends before *vng28*.
Chromosome	~25,216	TSD																	TSD: intergenic	Starts after *vng29* and ends before *vng30*.
Chromosome	~29,154	TSD																	TSD: coding	In *vng32*.
Chromosome	~48,587	Δ~500 bp																	ISH8-3 mediated	Starts before *vng52* and ends in *vng53*.
Chromosome	~52,664	TSD																	TSD: intergenic	Starts after *vng56* and ends before *vng57*.
Chromosome	~181,512	TSD																	TSD: coding	In *dph* (Putative DNA primase/helicase - phage associated).
Chromosome	414,229	C→A																	A675A (GCG→GCT)	In *vng537* (TRAP transporter permease).
Chromosome	~749,543	TSD																	TSD: coding	In *vng985*.
Chromosome	~753,552	TSD and Δ1bp																	TSD: intergenic and $(T)_{8\rightarrow8}$	Starts after *vng987* and ends before *vng988* (hypothetical protein/DUF2085 domain-containing protein).
Chromosome	~754,476	TSD																	TSD: coding	In *xcd* (integrase).
Chromosome	~772,459	TSD																	TSD: intergenic	Starts before *vng1007* and ends before *flaA1a* (flagellin A1 precursor).
Chromosome	~1,089,129	TSD																	TSD: coding	**In *bop* (rhodopsin).**
Chromosome	~1,229,749	TSD/Δ																	TSD: coding/ ISH2 deletion	In *vng1650*.
PNRC100	0	Δ~7500 bp																	ISH7-1 deleted	Starts before *vng5001*, *vng5003*, *vng5005*, *vng5007*, *vng5008*, *vng5009*, *sojA* (*spo0*A activation inhibitor), ends in *vng5011*.
PNRC100	~9,546	Δ~2000 bp																	ISH3-1	Starts in *repH* (replication protein), ends after *repH*.
PNRC100	~14,052	Δ~147 bp																	ISH3-1	Starts after *vng5015* and ends before *vng5016*.
PNRC100	~15,600	Δ16500 bp																	ISH8-3, 8-1	Starts before *vng5016*, *vng5017*, *gvpM-L1-K1-J1-I1-H1-G1-F1-E1-D1-A1-C1-N1-O1* (GvpM protein cluster A), *sojB* (Spo0A activation inhibitor), *htlD* (Htr-like protein), *vng5038*, *tbpA* (transcription initiation factor IID), ends after *vng5040*.
PNRC100	~41,820	Δ~17000bp																	ISH5-1*, 8-5	Starts before *cydAB* (cytochrome d oxidase), *vng5059*, *vng5061*, *vng5062*, *vng5063*, *vng5064*, *phoT1* (Na dep. phosphate transporter), *boa3* (bacterio-opsin activator), *vng5069*, *yfmO3* (MDR, *vng5073*, *vng5074*, *vng5075*, *trxA-trxB1-trh* (thioredoxin reductase related), *vng5079*, *vng5080*, ends after *vng5081*.
PNRC100	~71,208	Δ~3447 bp																	ISH2	Starts before *vng5097*, *yobE* (general secretion pathway), ends in *vng5100*.
PNRC100	~75,169	Δ~4534 bp																	ISH2	Starts in *vng5102*, *vng5104*, *vng5105*, *vng5106*, ends after *vng5108* (putative winged helix DBD - Bonneau et al 2004).
PNRC100	~81,100	Δ~750 bp																	ISH8-3, 3-1	Starts before and ends after *vng5112*.
PNRC100	~83,375	Δ~3790 bp																	ISH3-1, 7-2	Starts before *vng5115*, *vng5116*, *vng5118*, *vng5119*, *vng5120*, and ends in *vng5122*.
PNRC100	~87,224	SNP																	SNP	In *vng5122*.
PNRC100	~133,744	Δ~8776 bp																	ISH8-2, 3-3	Starts before *vng5173*, *vng5174*, *vng5175*, mth (putative methyltransferase), *arsR2* (transcriptional regulator), *vng5178*, *arsA2* (arsenical pump-driving ATPase), *arsD* (arsenic resistance repressor), *arsR* (transcriptional regulator), *arsC* (transcriptional regulator), and ends after *vng5185*.
PNRC100	~143,907	Δ~6349 bp																	ISH3-3, 2	Starts before *vng 5186*, *vng5189*, *vng5191*, *vng5192*, *rfa1* (single-stranded DNA-binding replication protein A), *vng5195*, and ends in *vng5197*.
PNRC100	~150,769	Δ~109 bp																	ISH2, 3-2	Starts after *vng5198* and ends before *vng5199*.
PNRC100	~152,257	Δ~13 bp																	ISH2, 3-2	Starts and ends in *vng5199*.
PNRC100	~153,526	Δ~15 bp																	ISH3-2, 2	Starts after *vng5200* and ends before *vng5201*.
PNRC100	~164,889	Δ16,681 bp																	ISH8-5, 5-1	Starts before *vng5216*, *vng5217*, *vng5218*, *trxA-trxB1-trh* (thioredoxin reductase related, *vng522*, *vng5223*, *vng5224*, *yfmO3* (MDR protein), *vng5228*, *boa3* (bacterio-opsin activator), *phoT1* (Na dep. phosphate transporter), *vng5233*, *vng5234*, *vng5235*, *vng5236*, *vng5238*, *cydBA* (cytochrome d oxidase).

PNRC200	0	Δ~7760 bp																	ISH 7-1 deleted	Starts before *vng6001, vng6003, vng6005, vng6007, vng6008, vng6009, sojA* (*spo0A* activation inhibitor), ends in *vng6011*.
PNRC200	~7,477	TSD																	TSD: coding	In *vng6011*.
PNRC200	~9,569	Δ2000 bp																	ISH 3-1	Starts in *repH* (replication protein), ends before *vng6015*.
PNRC200	~14052	Δ~143 bp																	ISH 3-1	Starts and ends before *vng6016*.
PNRC200	~15,594	Δ16447 bp																	ISH 8-3, 8-1	Starts before *vng6017*, gvpM-L1-K1-J1-I1-H1-G1-F1-E1-D1-A1-C1-N1-O1 (GvpM protein cluster A), *sojB* (Spo0A activation inhibitor), *htlD* (Htr-like protein), *vng6036, tbpA* (transcription initiation factor IID), *vng6038,* ends before *vng6039*.
PNRC200	~41,819	Δ~16682 bp																	ISH 5-1*, 8-5	Starts before *cydAB* (cytochrome d oxidase), *vng6057, vng6059, vng6060, vng6061.vng6062, phoT1* (Na-dep. phosphate transporter), *boa3* (bacterio-opsin activator), *vng6066, yfmO3* (MDR homolog), *vng6070, vng6071, arlR18* (transcription regulator), *trxA-trxB1-trh (thioredoxin reductase related*), *xcd* (integrase/recombinase), *vng6077, vng6078,* ends before *vng6079*.
PNRC200	~71,208	Δ~3447 bp																	ISH 2	Starts before *vng6094, yobE* (general secretion pathway), ends in *vng6097*.
PNRC200	~75,168	Δ~3905 bp																	ISH 2, 8-4	Starts in *vng6099, vng6101, vng6102, vng6103,* ends before *vng6105.*
PNRC200	~81,101	Δ~874 bp																	ISH 8-4, 3-1	Starts before *vng6109,* ends before *vng6111*.
PNRC200	~83,374	Δ~4648 bp																	ISH 3-1, 7-2	Starts before *xcd* (integrase/recombinase), includes *vng6113, vng6115, vng6116, vng6117,* ends in *vng6119*.
PNRC200	~87,224	SNP																	V→L(GTG→CTG)	In *vng6119.*
PNRC200	~138,366	Δ16038 bp																	ISH 8-4	Starts in *vng6162, vng6163, orc2* (*orc*/cell division control protein 6), *vng6165, nbp2* (nucleic acid binding protein), *vng6168, vng6170, vng6171, srl1* (*smc* and *rad50* like ATPase), *trkA2* (TRK potassium uptake system protein), *kdpABC* (potassium-transporting ATPase), *cat3* (cationic amino acid transporter), *vng6180,* ends in *vng6181*.
PNRC200	~140,521	12 bp (1→2)																	TSD: coding	Starts and ends in *orc2* (*orc*/cell division control protein 6).
PNRC200	~244,149	TSD																	TSD: coding	**Starts and ends in *nhaC3* (Na+/H+ antiporter).**
PNRC200	~248,490	TSD																	TSD: coding	Starts and ends in *arcR* (transcription regulator).
PNRC200	~262,599	Δ2839 bp																	ISH 3-2, 8-3 / ISH 8-3 deleted	Starts before *vng6329* and ends after *vng6330.*
PNRC200	~272,000	Δ958 bp																	ISH 6, 3-2	Starts after *vng6431* and ends before *vng6343.*
PNRC200	~274,345	Δ2289 bp																	ISH 3-2, 8-4	Starts before *vng6343* and ends after *vng6344.*
PNRC200	~278,031	Δ30707 bp																	ISH 8-4, 2	Starts in *vng6346, vng6348, vng6349, tfbC* (transcription initiation factor IIB, *vng6353, comA* (competence-like protein), *vng6355. vng6357, vng6359, tnp2, polB2* (DNA polymerase B2), *orc4* (*orc*/cell division control protein 6), *vng6364, vng6365, vng6366, vng6367, vng6368, vng6370, mmr* (Mrr restriction), *vgn6372, phrH* (PhiH1 repressor homolog), *vng6375, vng6377, vng6378, fes* (putative iron-sulfur protein), *vng6381, lctP* (L-lactate permease), *vng6384, vng6385, ab1R1* (transcriptional regulator), *tfbE* (TI factor IIB), ends in *vng6390*.
PNRC200	~278,118	TSD																	TSD: coding	Starts and ends in *vng6345.*
PNRC200	~279,927	TSD																	TSD: intergenic	Starts after *vng6348* and ends before *vng6349.*
PNRC200	~293,402	TSD																	TSD: coding	Starts and ends in *vng6364.*
PNRC200	~309,253	Δ~560 bp																	ISH 2, 8-3	Starts before *vng6393* and ends before *vng6395.*
PNRC200	~311,206	Δ~12115 bp																	ISH 8-3, 11	Starts before *nbp3* (nucleic acid binding protein), *vng6397, vng6400, vng6401, arlR20* (transcriptional regulator), *rfa6* (replication factor A related protein - *rfa32*), *vng6404, vng6406, vng6407, phzF, vng6409, vng6411, vng6412, vng6413, vng6416, vng6418, vng6419,* ends after *vng6420*.
PNRC200	~324,384	Δ~8409 bp																	ISH 11	Starts before *vng6424, vng6427, vng6429, vng6430, vng6431, vng6432, vng6434, tbpF* (transcription initiation factor IID), *vng6439,* ends after *vng6441*.

* "Annotation" column code: "ISH *** mediated" = flanking ISH elements, if relevant, TSD = target site duplication of ISH element insertion, missense mutations in blue, silent mutations in green, nonsense mutation = "nonsense".

"Gene" column code: (mutation starts or ends before this gene name), → ← indicates gene directionality, [mutation starts, ends, or is entirely contained within this gene name], "-" indicates intervening omitted genes found in description, "/" indicates mutation is between two genes.

ǂThis chart does not indicate shared lineage through identical mutations. Genes listed here are impacted by evolution in multiple strains by similar mutation types only. For a complete list of mutations, see **Tables S1-S3.**

Table 3. Classes of mutations found in evolved clones.*

Chromosome																	
	Low pH				Control				Low pH and iron-rich				Iron-rich				
Mutation Type	J1	J2-1	J3-1	J4-2	M1	M2-2	M3-1	M4-1	K1	K2-1	K3	K4	S1	S2	S3	S4	Mutation Sum
TSD	4	5	3	5	1	4	4	1	7	6	5	5	1	6	6	1	**64**
Deletion	1	1	0	1	1	1	2	2	1	1	0	1	0	0	1	0	**13**
SNP	0	0	1	0	1	2	1	1	1	1	0	1	0	0	0	1	**10**
Insertion	0	0	0	0	0	0	0	0	0	0	0	0	0	0	0	0	**0**
Chromosome Total	**5**	**6**	**4**	**6**	**3**	**7**	**7**	**4**	**9**	**8**	**5**	**7**	**1**	**6**	**7**	**2**	**87**

PNRC100																	
Mutation Type	J1	J2-1	J3-1	J4-2	M1	M2-2	M3-1	M4-1	K1	K2-1	K3	K4	S1	S2	S3	S4	Mutation Sum
TSD	0	1	0	0	0	7	0	0	3	0	0	0	2	2	0	0	**15**
Deletion	5	3	4	7	2	0	6	3	17	8	8	10	4	3	5	4	**89**
SNP	2	0	0	0	0	6	0	0	0	0	3	5	0	0	0	0	**16**
Insertion	0	0	0	0	0	0	0	0	0	0	0	0	0	0	0	0	**0**
PNRC100 Total	**7**	**4**	**4**	**7**	**2**	**13**	**6**	**3**	**20**	**8**	**11**	**15**	**6**	**5**	**5**	**4**	**120**

PNRC200																	
Mutation Type	J1	J2-1	J3-1	J4-2	M1	M2-2	M3-1	M4-1	K1	K2-1	K3	K4	S1	S2	S3	S4	Mutation Sum
TSD	1	1	2	1	1	4	0	0	3	7	3	7	2	0	3	5	**40**
Deletion	6	4	6	7	8	14	15	7	15	5	4	5	3	5	6	5	**115**
SNP	1	0	0	0	0	5	0	0	1	0	3	5	0	0	0	0	**15**
Insertion	1	0	0	0	0	0	0	0	0	0	0	0	0	0	0	0	**1**
PNRC200 Total	**9**	**5**	**8**	**8**	**9**	**23**	**15**	**7**	**19**	**12**	**10**	**17**	**5**	**5**	**9**	**10**	**171**

Complete genome																	
Mutation Type	J1	J2-1	J3-1	J4-2	M1	M2-2	M3-1	M4-1	K1	K2-1	K3	K4	S1	S2	S3	S4	Mutation Sum
TSD	5	7	5	6	2	15	4	1	13	13	8	12	5	8	9	6	**119**
Deletion	12	8	10	15	11	15	23	12	33	14	12	16	7	8	12	9	**217**
SNP	3	0	1	0	1	13	1	1	2	1	6	11	0	0	0	1	**41**
Insertion	1	0	0	0	0	0	0	0	0	0	0	0	0	0	0	0	**1**
Complete Total	**21**	**15**	**16**	**21**	**14**	**43**	**28**	**14**	**48**	**28**	**26**	**39**	**12**	**16**	**21**	**16**	**378**

*TSD = target site duplication; SNP = single nucleotide polymorphism.

Table 4. Coverage depth for NRC-1 and evolved clones.

Strain	Main chromosome		pNRC100		pNRC200	
	Read depth*	SD	Read depth*	SD	Read depth*	SD
NRC-1	50	10	128	15	64	10
J1	46	9	338	29	53	9
J2-2	41	9	156	14	48	8
J3-1	57	11	87	13	91	14
J4-2	64	11	137	15	85	13
M1	49	9	187	18	44	7
M2-2	67	11	165	17	62	10
M3-1	49	10	275	26	54	9
M4-1	65	11	162	13	75	11
K1	74	13	72	10	63	11
K2-1	72	13	NA	NA	76	11
K3	52	10	363	29	92	13
K4	59	11	96	11	71	15
S1	39	8	125	15	44	8
S2	42	9	169	18	34	7
S3	47	10	202	16	55	9
S4	46	9	185	14	37	7

*Mean copy number of sequence across the replicon, according to the *breseq* fitted dispersion model. SD = standard deviation predicted by the model.

Table 5. ISH insertions confirmed by PCR in acid-adapted strains.

Strain	Gene Mutation	ISH	Primer 1	Primer 2
J1	*nha*C3 insertion	ISH4	GATAACGATGGACATGTACT	GTCGGTATCGTTCTTTTGGG
J3-1	*bop* insertion	ISH1	GAGTTACACACATATCCTCG	GCGTAGAATTTCTTTGCATC
J4-2	*nhaC3* insertion	ISH11	GATAACGATGGACATGTACT	GTCGGTATCGTTCTTTTGGG
K1	*nhaC3* insertion	ISH2	GATAACGATGGACATGTACT	GTCGGTATCGTTCTTTTGGG
K2-1	*nhaC3* insertion	ISH4	GATAACGATGGACATGTACT	GTCGGTATCGTTCTTTTGGG
K3	*nhaC3* insertion	ISH4	GATAACGATGGACATGTACT	GTCGGTATCGTTCTTTTGGG
K4	*nhaC3* insertion	ISH2	GATAACGATGGACATGTACT	GTCGGTATCGTTCTTTTGGG

Table 6. Acid-evolved clone J3-1 mutations.* ‡

Replicon	Start bp	End bp	Mutation	Annotation	Gene	Description
Chromosome	749,943	749,954	(11 bp) 1→2	TSD: coding (562/2007 nt)	*[vng985→]*	In *vng985.*
Chromosome	1,089,129	1,089,137	(8 bp) 1→2	TSD: coding (15/789 nt)	*[bop→]*	In *bop* (rhodopsin).
Chromosome	1,163,363		A→G	K197R (AAA→AGA)	*[vng1561→]*	In *vng1561* (ferredoxin).
Chromosome	1,229,749	1,229,760	(11 bp) 1→2	TSD: coding (582/849 nt)	*[vng1650←]*	In *vng1650.*
PNRC100	0	7,788	Δ7788 bp	ISH7-1 deleted	*(vng5001←) - [←vng5011]*	Starts before *vng5001*, includes *vng5003*, *vng5005*, *vng5007*, *vng5008*, *vng5009*, *sojA* (*spo0A* activation inhibitor), ends in *vng5011*.
PNRC100	71,210	74,656	Δ3447 bp	ISH2 mediated	*(vng5097→) - ←[vng5100]*	Starts before *vng5097*, includes *yobE* (general secretion pathway protein homolog), ends in *vng5100*.
PNRC100	133,743	142,521	Δ8779 bp	ISH8-2, 3-3 mediated	*(vng5173←) - (→vng5185)*	Starts before *vng5173*, includes *vng5174*, *vng5175*, mth (putative methyltransferase), *arsR2* (transcriptional regulator), *vng5178*, *arsA2* (arsenical pump-driving ATPase), *arsD* (arsenic resistance repressor), *arsR* (transcriptional regulator), *arsC* (transcriptional regulator), and ends after *vng5185*.
PNRC100	143,909	150,253	Δ6345 bp	ISH3-3, 2 mediated	*(vng5186→) - [→vng5197]*	Starts before *vng 5186*, includes *vng5189*, *vng5191*, *vng5192*, *rfa1* (single-stranded DNA-binding replication protein A), *vng5195*, and ends in *vng5197*.
PNRC200	0	7,760	Δ7760 bp	ISH 7-1 deleted	*vng6001← - [←vng6011]*	Starts before *vng6001,* includes *vng6003, vng6005, vng6007, vng6008, vng6009, sojA* (*spo0A* activation inhibitor), ends in *vng6011*.
PNRC200	71,219	74,595	Δ3377 bp	ISH 2 mediated	*(vng6094→) - [←vng6097]*	Starts before *vng6094,* includes *yobE* (general secretion pathway homolog), ends in *vng6097*.
PNRC200	244,422	244,430	9 bp (1→2)	TSD: intergenic	*(nhaC3←) / (arcB←)*	Starts after *nhaC3* (Na+/H+ antiporter) and ends before *arcB* (ornithine carbamoyltransferase).
PNRC200	249,147	249,157	11 bp (1→2)	TSD: coding	*[arcR←]*	Starts and ends in *arcR* (transcription regulator).
PNRC200	262,603	265,437	Δ2835 bp	ISH 3-2, 8-3 mediated/ ISH 8-3 deleted	*(vng6329←) / (→vng6330)*	Starts before *vng6329* and ends after *vng6330*.
PNRC200	309,256	309,812	Δ557 bp	ISH 2, 8-3 mediated	*(vng6393←) - (←vng6395)*	Starts before *vng6393* and ends before *vng6395.*
PNRC200	311,213	323,320	Δ12108 bp	ISH 8-3, 11 mediated	*(nbp3→) - (←vng6420)*	Starts before *nbp3* (nucleic acid binding protein), includes *vng6397, vng6400, vng6401, arlR20* (transcriptional regulator), *rfa6* (replication factor A related protein - *rfa32*), *vng6404, vng6406, vng6407, phzF* (phenazine biosynthetic protein, *vng6409, vng6411, vng6412, vng6413, vng6416, vng6418, vng6419,* and ends after *vng6420*.
PNRC200	324,386	332,792	Δ8407 bp	ISH 11 mediated	*(vng6424←) - (→vng6441)*	Starts before *vng6424,* includes *vng6427, vng6429, vng6430, vng6431, vng6432, vng6434, tbpF* (transcription initiation factor IID), *vng6439,* and ends after *vng6441*.

* "Annotation" column code: "ISH *** mediated" = flanking ISH elements, if relevant, TSD = target site duplication of ISH element insertion, missense mutations in blue.
"Gene" column code: (mutation starts or ends before this gene name), → ← indicates gene directionality, [mutation starts, ends, or is entirely contained within this gene name], "-" indicates intervening omitted genes found in description, "/" indicates mutation is between two genes.
‡Highlight indicates mutation unique to J3-1.

Table 7: Change in gas vesicle phenotype during evolution across populations*

		Generation				
Media condition	**Strain**	**100**	**200**	**300**	**400**	**500**
pH 6.3 100 mM PIPES	**J1**	+	$Vac^{+/-}$	-	-	-
	J2	+	$Vac^{+/-}$	-	-	$Vac^{+/-}$
	J3	>1% Vac^{-}	$Vac^{+/-}$	-	-	$Vac^{+/-}$
	J4	+	+	-	-	$Vac^{+/-}$
pH 7.5 100 mM MOPS	**M1**	+	+	+	$Vac^{+/-}$	$Vac^{+/-}$
	M2	+	+	+	$Vac^{+/-}$	$Vac^{+/-}$
	M3	+	+	+	$Vac^{+/-}$	$Vac^{+/-}$
	M4	+	>1% Vac^{-}	+	+	$Vac^{+/-}$
pH 6.3 100 mM PIPES 600 µM $FeSO_4$	**K1**	+	$Vac^{+/-}$	-	$Vac^{+/-}$	$Vac^{+/-}$
	K2	$Vac^{+/-}$	$Vac^{+/-}$	-	-	$Vac^{+/-}$
	K3	+	$Vac^{+/-}$	-	-	$Vac^{+/-}$
	K4	+	$Vac^{+/-}$	-	-	$Vac^{+/-}$
pH 7.5 100 mM MOPS 600 µM $FeSO_4$	**S1**	+	+	-	-	-
	S2	+	+	-	-	-
	S3	+	+	-	-	-
	S4	+	+	+	-	-

* "+" indicates gas vesicle-forming, "–" indicates non gas vesicle-forming

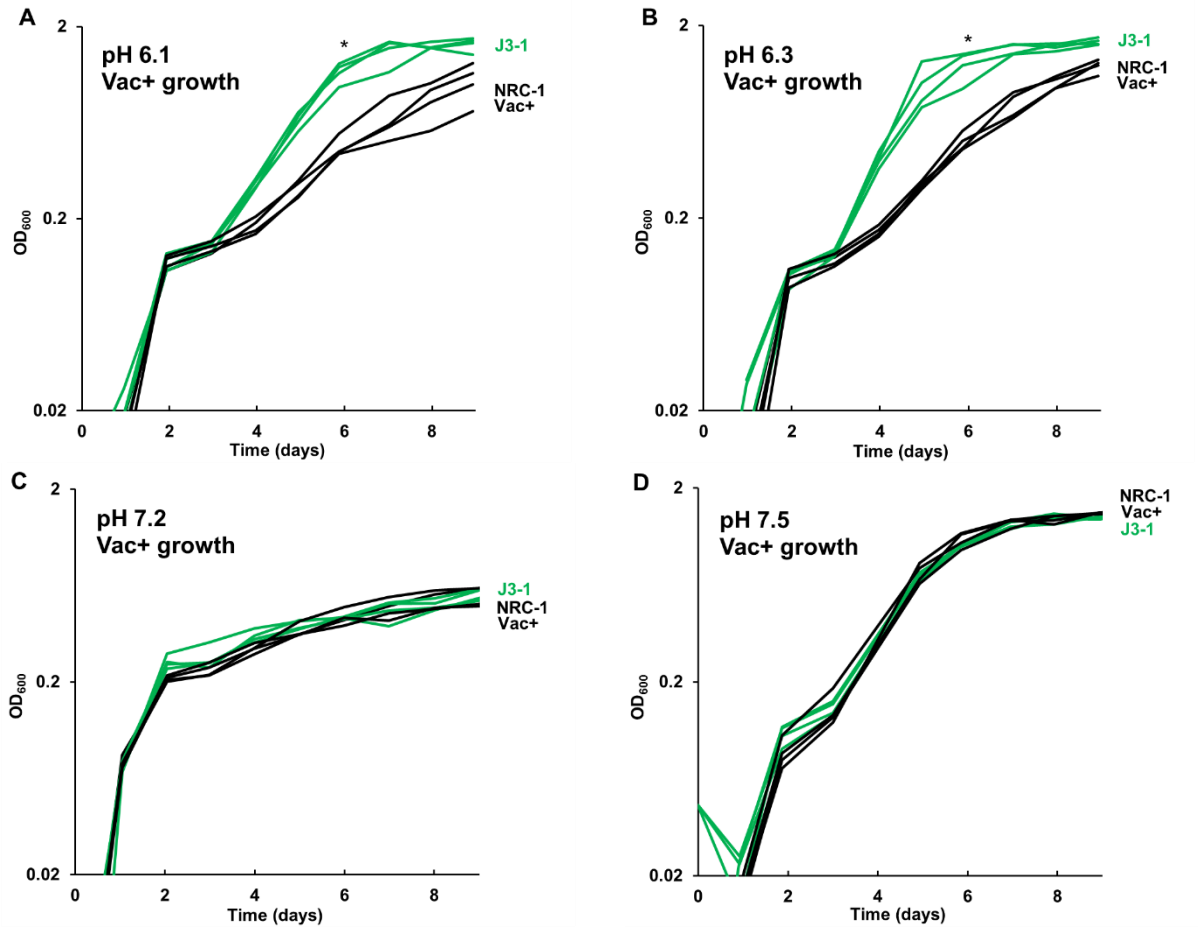

Figure 1. Acid-evolved clone J3-1 shows a pH-dependent growth rate increase compared to NRC-1. Growth medium was CM^+ buffered at (**A**) pH 6.1 with 100 mM PIPES; (**B**) pH 6.3 with 100 mM PIPES; (**C**) pH 7.2 with 100 mM MOPS; or (**D**) pH 7.5 with 100 mM MOPS. Representative curves of three replicates are shown. For J3-1 and NRC-1, the OD_{600} values at 144 h were compared by two-tailed t-test. At pH 6.1, P = 0.002; at pH 6.3, P = 0.01; at pH 7.2, P = 0.91; at pH 7.5, P = 0.45. "*" indicates significant endpoint growth increase from NRC-1 ancestor in at least 2 replicates.

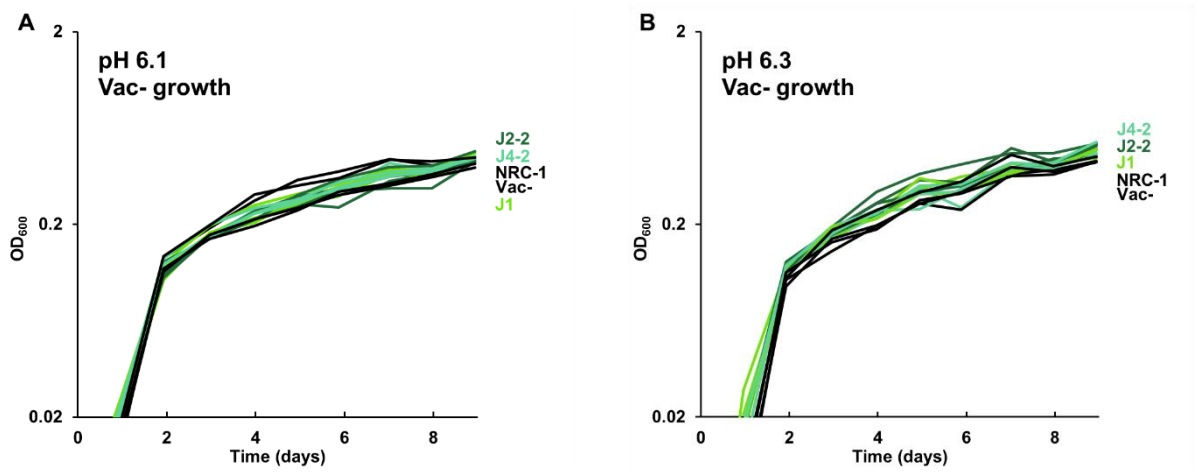

Figure 2. Growth of acid-evolved clones J1, J2-2, J4-2. Growth medium was CM^+ pH 6.3 with 100 mM PIPES, at (**A**) pH 6.1, (**B**) pH 6.3. Cultures were diluted from a 7-day culture in CM^+ pH 7.2. Gas vesicle-deficient clones were compared to gas vesicle-deficient ancestral mutant NRC-1 and cell density values post log-phase (OD_{600} at 6 days) were analyzed using ANOVA with Tukey post-hoc. Representative curves of three replicates are shown.

REFERENCES

1. Oren A. 2013. Life at high salt concentrations, intracellular KCl concentrations, and acidic proteomes. Front Microbiol 4:1–6.
2. Reysenbach A, Pace NR. 1995. Archaea: A laboratory manual - Halophiles. Cold Spring Harbor Laboratory Press, Cold Spring Harbor.
3. Ng W V., Kennedy SP, Mahairas GG, Berquist B, Pan M, Shukla HD, Lasky SR, Baliga NS, Thorsson V, Sbrogna J, Swartzell S, Weir D, Hall J, Dahl TA, Welti R, Goo YA, Leithauser B, Keller K, Cruz R, Danson MJ, Hough DW, Maddocks DG, Jablonski PE, Krebs MP, Angevine CM, Dale H, Isenbarger TA, Peck RF, Pohlschroder M, Spudich JL, Jung K-H, Alam M, Freitas T, Hou S, Daniels CJ, Dennis PP, Omer AD, Ebhardt H, Lowe TM, Liang P, Riley M, Hood L, DasSarma S. 2000. Genome sequence of *Halobacterium* species NRC-1. Proc Natl Acad Sci 97:12176–12181.
4. Kish A, Kirkali G, Robinson C, Rosenblatt R, Jaruga P, Dizdaroglu M, Diruggiero J. 2009. Salt shield: Intracellular salts provide cellular protection against ionizing radiation in the halophilic archaeon, *Halobacterium salinarum* NRC-1. Environ Microbiol 11:1066–1078.
5. Jones DL, Baxter BK. 2017. DNA repair and photoprotection: Mechanisms of overcoming environmental ultraviolet radiation exposure in halophilic archaea. Front Microbiol 8:1882.
6. Coker JA, DasSarma P, Kumar J, Müller JA, DasSarma S. 2007. Transcriptional profiling of the model archaeon *Halobacterium* sp. NRC-I: Responses to changes in salinity and temperature. Saline Systems 3:doi:10.1186/1746-1448-3-6.
7. Wang G, Kennedy SP, Fasiludeen S, Rensing C, DasSarma S. 2004. Arsenic resistance in *Halobacterium* sp. strain NRC-1 examined by using an improved gene knockout system. J Bacteriol 186:3187–3194.
8. DasSarma P, Tuel K, Nierenberg SD, Phillips T, Pecher WT, Nrc- H, Nierenberg SD, DasSarma S. 2016. Inquiry-driven teaching & learning using the archaeal microorganism Halobacterium. Am Biol Teach 78:7–13.
9. DasSarma S. 2006. Extreme halophiles are models for astrobiology. Microbe 1:120–126.
10. Leuko S, Domingos C, Parpart A, Reitz G, Rettberg P. 2015. The survival and resistance of *Halobacterium salinarum* NRC-1, *Halococcus hamelinensis*, and *Halococcus morrhuae* to simulated outer space solar radiation. Astrobiology 15:987–997.
11. DasSarma P, Laye VJ, Harvey J, Reid C, Shultz J, Yarborough A, Lamb A, Koske-Phillips A, Herbst A, Molina F, Grah O, Phillips T, DasSarma S. 2017. Survival of halophilic archaea in Earth's cold stratosphere. Int J Astrobiol 16:321–327.
12. DasSarma P, DasSarma S. 2018. Survival of microbes in Earth's stratosphere. Curr Opin Microbiol 43:24–30.
13. Madden MEE, Bodnar RJ, Rimstidt JD. 2004. Jarosite as an indicator of water- limited chemical weathering on Mars. Nature 431:821–823.
14. Pritchett BN, Elwood Madden ME, Madden AS. 2014. Jarosite dissolution rates and maximum lifetimes in high salinity brines: Implications for Earth and Mars. Earth Planet Sci Lett 391:67–68.
15. Dopson M, Ossandon FJ, Lövgren L, Holmes DS. 2014. Metal resistance or tolerance? Acidophiles confront high metal loads via both abiotic and biotic mechanisms. Front Microbiol 5:doi: 10.3389/fmicb.2014.00157.

16. Moran-Reyna A, Coker JA. 2014. The effects of extremes of pH on the growth and transcriptomic profiles of three haloarchaea. F1000 Res 3:1–15.
17. Lenski RE, Travisano M. 1994. Dynamics of adaptation and diversification: A 10,000-generation experiment with bacterial populations. Proc Natl Acad Sci U S A 91:6808–14.
18. Lenski RE, Rose MR, Simpson SC, Tadler SC. 1991. Long-term experimental evolution in *Escherichia coli*. I. Adaptation and divergence during 2,000 generations. Am Nat 138:1315–1341.
19. Tenaillon O, Barrick JE, Ribeck N, Deatherage DE, Blanchard JL, Dasgupta A, Wu GC, Schneider D, Lenski RE. 2016. Tempo and mode of genome evolution in a 50,000 -generation experiment. Nature 536:165–170.
20. Creamer KE, Ditmars FS, Basting PJ, Kunka KS, Hamdallah IN, Bush SP, Scott Z, He A, Penix SR, Gonzales AS, Eder EK, Camperchioli DW, Berndt A, Clark MW, Rouhier KA, Slonczewski JL. 2017. Benzoate- and salicylate-tolerant strains of *Escherichia coli* K-12 lose antibiotic resistance during laboratory evolution. Appl Environ Microbiol 83:e02736.
21. He A, Penix SR, Basting PJ, Griffith JM, Creamer KE, Camperchioli D, Clark MW, Gonzales AS, Erazo JSC, George NS, Bhagwat AA, Slonczewski JL. 2017. Acid evolution of *Escherichia coli* K-12 eliminates amino acid decarboxylases and reregulates catabolism. Appl Environ Microbiol 83:e00442-17.
22. Harden MM, He A, Creamer K, Clark MW, Hamdallah I, Martinez KA, Kresslein RL, Bush SP, Slonczewski JL. 2015. Acid-adapted strains of *Escherichia coli* K-12 obtained by experimental evolution. Appl Environ Microbiol 81:1932–1941.
23. Schou MF, Kristensen TN, Kellermann V, Schlötterer C, Loeschcke V. 2014. A *Drosophila* laboratory evolution experiment points to low evolutionary potential under increased temperatures likely to be experienced in the future. J Evol Biol 27:1859–1868.
24. Slonczewski JL, Fujisawa M, Dopson M, Krulwich TA. 2009. Cytoplasmic pH measurement and homeostasis in bacteria and archaea., p. 1–79, 317. *In* Advances in Microbial Physiology.
25. Kanjee U, Houry WA. 2013. Mechanisms of acid resistance in *Escherichia coli*. Annu Rev Microbiol 67:65–81.
26. Hamdallah I, Torok N, Bischof KM, Majdalani N, Chadalavada S, Mdluli N, Creamer KE, Clark M, Holdener C, Basting PJ, Gottesman S, Slonczewski JL. 2018. Experimental evolution of *Escherichia coli* K-12 at high pH and RpoS induction. Appl Environ Microbiol 84:e00520.
27. DeVeaux LC, Müller JA, Smith J, Petrisko J, Wells DP, DasSarma S. 2007. Extremely radiation-resistant mutants of a halophilic archaeon with increased single-stranded DNA-binding protein (RPA) gene expression. Radiat Res 168:507–514.
28. McCarthy S, Johnson T, Pavlik BJ, Payne S, Schackwitz W, Martin J, Lipzen A, Keffeler E, Blum P. 2016. Expanding the limits of thermoacidophily in the archaeon *Sulfolobus solfataricus* by adaptive evolution. Appl Environ Microbiol 82:857–867.
29. Ai C, McCarthy S, Eckrich V, Rudrappa D, Qiu G, Blum P. 2016. Increased acid resistance of the archaeon, *Metallosphaera sedula* by adaptive laboratory evolution. J Ind Microbiol Biotechnol 43:1455–1465.
30. Krulwich TA, Sachs G, Padan E. 2011. Molecular aspects of bacterial pH sensing and homeostasis. Nat Rev Microbiol 9:330–343.
31. Lund P, Tramonti A, De Biase D. 2014. Coping with low pH: Molecular strategies in neutralophilic bacteria. FEMS Microbiol Rev 38:1091–1125.

32. Simsek M, DasSarma S, RajBhandary U, Khorana H. 2006. A transposable element from *Halobacterium halobium* which inactivates the bacteriorhodopsin gene. Proc Natl Acad Sci 79:7268–7272.
33. Dummer AM, Bonsall JC, Cihla JB, Lawry SM, Johnson GC, Peck RF. 2011. Bacterioopsin-mediated regulation of bacterioruberin biosynthesis in *Halobacterium salinarum*. J Bacteriol 193:5658–5667.
34. Ito M, Guffanti AA, Zemsky J, Ivey DM, Krulwich TA. 1997. Role of the *nhaC*-encoded Na^+/H^+ antiporter of alkaliphilic *Bacillus firmus* OF4. J Bacteriol 179:3851–3857.
35. Padan E, Bibi E, Ito M, Krulwich TA. 2005. Alkaline pH homeostasis in bacteria: New insights. Biochim Biophys Acta - Biomembr 1717:67–88.
36. Ng WL, Ciufo SA, Smith TM, Bumgarner RE, Baskin D, Faust J, Hall B, Loretz C, Seto J, Slagel J, Hood L, DasSarma S. 1998. Snapshot of a large dynamic replicon in a halophilic archaeon: Megaplasmid or minichromosome? Genome Res 8:1131–1141.
37. DasSarma S. 1989. Mechanisms of genetic variability in *Halobacterium halobium*: The purple membrane and gas vesicle mutations. Can J Microbiol 35:65–72.
38. Sapienza C, Doolittle WF. 1982. Unusual physical organization of the *Halobacterium* genome. Nature 295:384–389.
39. Deatherage DE, Barrick JE. 2014. Identification of mutations in laboratory-evolved microbes from next-generation sequencing data using *breseq*. Methods Mol Biol 1151:165–188.
40. Deatherage DE, Traverse CC, Wolf LN, Barrick JE. 2015. Detecting rare structural variation in evolving microbial populations from new sequence junctions using *breseq*. Front Genet 5:1–16.
41. Barrick JE, Colburn G, Deatherage DE, Traverse CC, Strand MD, Borges JJ, Knoester DB, Reba A, Meyer AG. 2014. Identifying structural variation in haploid microbial genomes from short-read resequencing data using *breseq*. BMC Genomics 15:1039.
42. DasSarma S, Halladay JT, Jones JG, Donovan JW, Giannasca PJ, de Marsac NT. 1988. High-frequency mutations in a plasmid-encoded gas vesicle gene in *Halobacterium halobium*. Proc Natl Acad Sci U S A 85:6861–5.
43. Ng WL, DasSarma S. 1991. Physical and genetic mapping of the unstable gas vesicle plasmid in Halobacterium halobium NRC-1, p. 305–311. *In* Rodriguez-Valera, F (ed.), General and Applied Aspects of Halophilic Microorganisms. Plenum Press.
44. Ng WL, Kothakota S, DasSarma S. 1991. Structure of the gas vesicle plasmid in Halobacterium halobium: Inversion isomers, inverted repeats, and insertion sequences. J Bacteriol 173:1958–1964.
45. Ng WL, Arora P, DasSarma S. 1993. Large deletions in class III gas vesicle-deficient mutants of *Halobacterium halobium*. Syst Appl Microbiol 16:560–568.
46. Pfeiffer F, Schuster SC, Broicher A, Falb M, Palm P, Rodewald K, Ruepp A, Soppa J, Tittor J, Oesterhelt D. 2008. Evolution in the laboratory: The genome of *Halobacterium salinarum* strain R1 compared to that of strain NRC-1. Genomics 91:335–346.
47. Soppa J. 2013. Evolutionary advantages of polyploidy in halophilic archaea. Biochem Soc Trans 41:339–343.
48. DasSarma S, Arora P. 1997. Genetic analysis of the gas vesicle gene cluster in haloarchaea. FEMS Microbiol Lett 153:1–10.
49. DasSarma P, Zamora RC, Müller JA, DasSarma S. 2012. Genome-wide responses of the model archaeon *Halobacterium* sp. strain NRC-1 to oxygen limitation. J Bacteriol

194:5530–5537.
50. DasSarma S, Arora P, Lin F, Molinari E, Yin LRS. 1994. Wild-type gas vesicle formation requires at least ten genes in the gvp gene cluster of *Halobacterium halobium* plasmid pNRC100. J Bacteriol 176:7646–7652.
51. Ruepp A, Soppa J. 1996. Fermentative arginine degradation in *Halobacterium salinarium* (formerly *Halobacterium halobium*): Genes, gene products,and transcripts of the *arcRACB* gene cluster. J Bacteriol 178:4942–4947.
52. Wimmer F, Oberwinkler T, Bisle B, Tittor J, Oesterhelt D. 2008. Identification of the arginine/ornithine antiporter ArcD from *Halobacterium salinarum*. FEBS Lett 582:3771–3775.
53. Gong S, Richard H, Foster JW. 2003. YjdE (AdiC) is the arginine:agmatine antiporter essential for arginine-dependent acid resistance in *Escherichia coli*. J Bacteriol 185:4402–4409.
54. Griffith JM, Basting PJ, Bischof KM, Wrona EP, Kunka KS, Tancredi A, Moore JP, Hyman M, Slonczewski JL. 2019. Experimental evolution of *Escherichia coli* K-12 in the presence of proton motive force (PMF) uncoupler carbonyl cyanide m-chlorophenylhydrazone selects for mutations affecting PMF-driven drug efflux pumps. Appl Environ Microbiol 85:e02792-18.
55. Redder P, Garrett RA. 2006. Mutations and rearrangements in the genome of *Sulfolobus solfataricus* P2. J Bacteriol 188:4198–4206.
56. Berquist BR, Müller JA, DasSarma S. 2006. 27 genetic systems for halophilic archaea. Methods Microbiol 35:649–680.
57. Thorvaldsdóttir H, Robinson JT, Mesirov JP, Thorvaldsdóttir H, Robinson JT, Mesirov JP. 2013. Integrative genomics viewer (IGV): High-performance genomics data visualization and exploration. Brief Bioinform 14:178–192.